

Demagnetization cooling of a gas

M. FATTORI*, T. KOCH, S. GOETZ, A. GRIESMAIER, S. HENSLER, J. STUHLER AND T. PFAU*

5. Physikalisches Institut, Universität Stuttgart, Pfaffenwaldring 57, 70550 Stuttgart, Germany

*e-mail: m.fattori@physik.uni-stuttgart.de; t.pfau@physik.uni-stuttgart.de

Published online: 29 October 2006; doi:10.1038/nphys443

Adiabatic demagnetization is an efficient technique for cooling solid samples by several orders of magnitude in a single cooling step. In gases, the required coupling between dipolar moments and motion is typically too weak, but in dipolar gases—of high-spin atoms or heteronuclear molecules with strong electric dipole moments, for example—the method should be applicable. Here, we demonstrate demagnetization cooling of a gas of ultracold ^{52}Cr atoms. Demagnetization is driven by inelastic dipolar collisions, which couple the motional degrees of freedom to the spin degree. In this way, kinetic energy is converted into magnetic work, with a consequent temperature reduction of the gas. Optical pumping is used to magnetize the system and drive continuous demagnetization cooling. We can increase the phase-space density of our sample by up to one order of magnitude, with almost no atom loss, suggesting that the method could be used to achieve quantum degeneracy via optical means.

Adiabatic demagnetization of a paramagnetic salt is the oldest method for reaching temperatures significantly below 1 K in solids¹. Although realized for the first time in the 1930s (ref. 2), this technique is still used today because of its simplicity and flexibility. Nuclear demagnetization refrigerators, which are based on the same principle of operation, use nuclear instead of electronic magnetic dipole moments³. Such refrigerators are crucial for studies on magnetic phases in solids as they allow the nuclear spin system to be cooled well below 1 μK (refs 4,5). Also known as the magnetocaloric effect⁶, demagnetization cooling works in paramagnetic materials. Such materials comprise particles with a total angular momentum quantum number J and a permanent magnetic dipole $g\mu(J(J+1))^{1/2}$, where μ is the unit of magnetic moment (μ_{B} for electrons and μ_{N} for nuclei) and $g > 0$ is the spectroscopic splitting factor. If an external magnetic field is applied, these dipoles will try to minimize their energy by aligning with the field and consequently, by generating a macroscopic magnetization M of the material. Quantum mechanically, this can be easily explained by looking at the imbalance in the occupation probability $\propto \exp(-E(m_j)/k_{\text{B}}T)$ of all the Zeeman states with energy $E(m_j) = g\mu B m_j$, where $m_j = -J, -J+1, \dots, J-1, J$ is the projection of the dipole moment along the magnetic field, k_{B} is Boltzmann's constant and T is temperature. For an intense magnetic field, where $g\mu B \gg k_{\text{B}}T$, the probability of occupation of the state $m_j = -J$ is nearly one and subsequently M saturates (see Fig. 1a). If the sample is isolated after this isothermal magnetization and B is reduced, the sample demagnetizes isoentropically, and in accordance with the state equation $dQ = TdS = 0 = dU + pdV - BdM$ (where Q is the heat added to the system, and S , U , p and V are the entropy, the internal energy, the pressure and the volume of the system respectively) we get $dU = BdM < 0$, as volume variations are negligible in a solid⁷. In other words, the system has to do magnetic work to drive the demagnetization and consequently the internal energy and therefore the temperature of the system decrease. The situation is illustrated in Fig. 1b. When $k_{\text{B}}T \approx g\mu B$, Zeeman states with $m_j > -J$ can be occupied at the expense of the energy of the external degrees of freedom of the particles in the solid. This leads to a net cooling effect. The cooling efficiency of this process can be understood by introducing the concept of the phonon reservoir, which includes the external degrees of freedom of the particles, and the spin reservoir to describe the internal state m_j . For high magnetic fields, the spin degree of freedom is frozen and the spin-reservoir specific heat c_s is negligible. The initial total energy E_i is then equal to the phonon-reservoir specific heat c_p times the initial temperature T_i . When

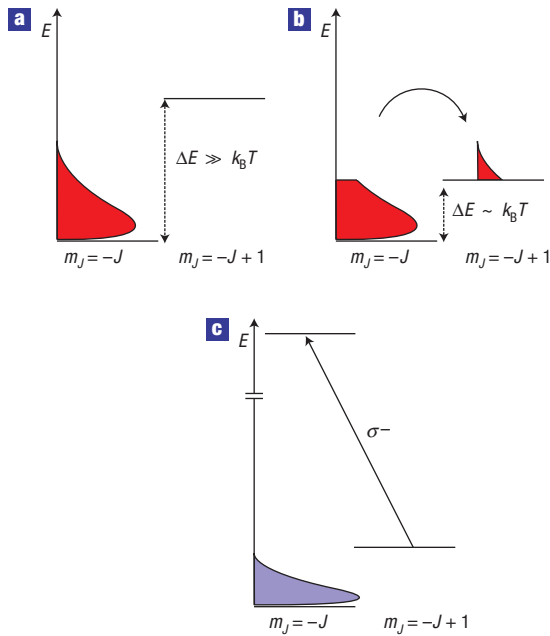


Figure 1 Illustration of demagnetization cooling. **a**, Initially the particles are polarized in the Zeeman state $m_J = -J$ at high magnetic field B . The mean energy $k_B T$ is well below the Zeeman energy separation $\Delta E = g\mu_B B$. **b**, Reducing the external magnetic field until $k_B T \approx g\mu_B B$ allows demagnetization of the system. Part of the energy of the sample is transferred into Zeeman energy with a net cooling effect. **c**, In an atomic gas, it is possible to use optical pumping to polarize the atoms back to $m_J = -J$, leaving the temperature nearly unchanged. The system is then ready for another cooling cycle.

$k_B T \approx g\mu_B B$, c_s becomes close to the value of k_B and, if a coupling between the two reservoirs exists, E_i must redistribute over a system with a total specific heat $c_p + c_s$. The final temperature is then

$$T_f = T_i \frac{c_p}{c_p + c_s} \quad (1)$$

Because in solids $c_p \ll c_s$, this implies that demagnetization can cool the sample by several orders of magnitude.

Despite being suggested by Kastler⁸ 25 years before the first proposal of laser cooling⁹, so far, demagnetization processes have not been implemented in cooling techniques for gases. This is mainly due to the very weak coupling between the spin and the external degrees of freedom (phonon) reservoir in a system where the density is much smaller than in a solid. Very recently, our group has revisited this old idea and quantitatively analysed its feasibility for the cooling of atoms that show large inelastic relaxation rates between magnetic substates¹⁰. During such relaxation, the sum of the quantum numbers m_{j1} and m_{j2} of two colliding atoms is not conserved and the demagnetization of the sample is allowed. The magnetic dipole–dipole interaction can induce inelastic relaxations of a rate that drastically increases with the atomic magnetic moments. In particular, the cross-section for the inelastic single spin-flip (only one atom changes its m_j value by one) is proportional to J^3 (ref. 11). In ref. 10, particular attention has been paid to chromium atomic gases¹² because Cr atoms in the 7S_3 ground state possess a very large magnetic dipole moment of six Bohr magnetons. This is due to the spin of six unpaired electrons in the outer shells of these atoms. As a consequence, in chromium the cross-section for inelastic single spin-flips is a factor of ~ 200 larger than in alkali atoms ($S = J = 1/2$).

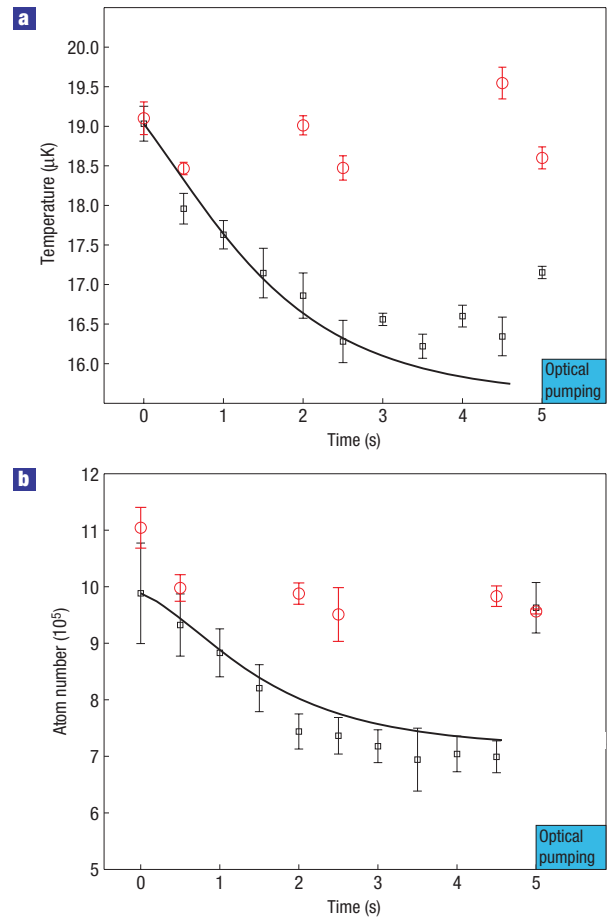


Figure 2 Single-step demagnetization. **a, b**, At time zero, the external magnetic field is suddenly switched from 1 G to 50 mG. The temperature (**a**) and atom number (**b**) evolution are represented by black squares. The red circles show how the system evolves if the external magnetic field is kept constant at 1 G. Every point is the result of the average of three measurements. The error bars are the standard deviation of the average. Demagnetization results in a temperature reduction and atomic depolarization, which our state-selective measurement clearly reveals. Switching on the OPB after 5 s slightly affects the temperature and pumps the atoms back to the initial state. The black curve is the result of a theoretical calculation that takes into account demagnetization through all seven magnetic sublevels. The only input parameters are the atom number, the initial temperature, the trap frequencies and the external magnetic field.

Here, we demonstrate demagnetization cooling of a gas for the first time. ^{52}Cr atoms in the 7S_3 ground state are initially polarized in the lowest-energy Zeeman state ($J = 3, m_j = -3$) with a magnetic splitting $2\mu_B B$ that is much larger than the temperature T of the sample. By reducing the magnetic field to values such that $3/2k_B T \approx 2\mu_B B$, transitions to higher energetic Zeeman substates, which are caused by dipolar relaxation collisions, cool the sample. In fact, the colliding atoms slow down because part of their kinetic energy is converted into Zeeman energy of the internal state. Single or double spin-flips are possible. The main advantage of demagnetization cooling in a gas is that by using optical pumping, it is possible to polarize the sample back to $m_j = -3$, thereby constantly cooling the spin reservoir (see Fig. 1c).

Our atoms are stored in an optical dipole trap that is realized by using a 1,064 nm fibre laser. A horizontal 20 W beam focused to a 30 μm waist generates a harmonic potential, independent of the magnetic substate, with trapping frequencies

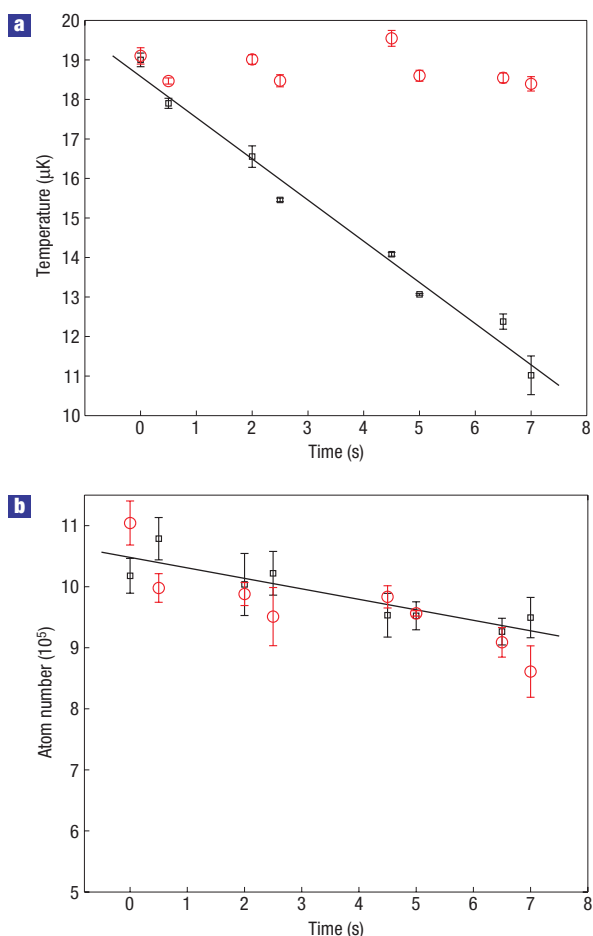


Figure 3 Continuous demagnetization cooling. **a,b**, The external magnetic field is linearly ramped from 250 mG to 50 mG in 7 s. The black squares show temperature **(a)** and atom number **(b)** evolution. The red circles show how the system evolves if the external magnetic field is kept at 1 G. Every point is the average of three measurements. The error bars are the standard deviation of the average. Note that the atom number reduction is not due to the cooling but due to single-particle losses probably associated with finite lifetime in the dipole trap. The lines through the data points are linear fits of the cooling measurements.

$\omega_x/2\pi = \omega_y/2\pi = 2$ kHz, $\omega_z/2\pi = 20$ Hz and a depth of 200 μ K. Our experiments start with 10^6 atoms polarized in $m_j = -3$. The details of the loading can be found in a previous report¹². The initial temperature of the sample (measured using absorption imaging and time-of-flight techniques) is 19 μ K due to plain evaporation and the external magnetic field is 1 G. If we suddenly decrease the magnetic field to 50 mG and allow the system to evolve, we observe a reduction of the temperature on a timescale of 3 s (see black squares in Fig. 2a). After 5 s, equilibrium is reached and we measure a final temperature of 16.5 μ K. We have repeated the measurement with a constant 1 G external magnetic field (see the red circles in Fig. 2a) and as expected, within the error bars (~ 0.5 μ K), no temperature reduction was detected.

As the energy of the atoms is much larger than $\hbar\omega_i$ ($i = x, y, z$), where \hbar is the reduced Planck constant, the gas can be described classically and the specific heat per particle of the external degrees of freedom reservoir is $3k_B$. Considering that the spin-reservoir contribution is of the order of k_B , we can then explain why a single-step demagnetization can reduce the temperature by about

25% (see equation (1)). Further proof of the demagnetization of the system comes from the atom number measurement. Our detection scheme makes use of σ^- light resonant with the $|^7S_3, m_j = -3\rangle \rightarrow |^7P_4, m'_j = -4\rangle$ transition. The level of light absorption depends on the atomic distribution over the Zeeman substates and is stronger for atoms polarized in $m_j = -3$ (for $m_j \neq -3$, we have a different Zeeman detuning and a different coupling strength to the $m'_j = m_j - 1$). As shown in Fig. 2b, demagnetization results in a reduction of the detected atom signal. To exclude the possibility of atom loss, after 5 s we repolarize the sample via optical pumping and check that the detection signal is still as large as it was at the beginning. The red circles in Fig. 2b show that this cooling step does not cause any significant atom loss with respect to the high magnetic field reference case. From the initial slope of the atom number and temperature curves in Fig. 2, it is possible to measure the depolarization rate at time $t = 0$

$$\frac{dN_{-3}}{dt} = -\beta_{dr} \frac{N_{-3}^2}{V},$$

where $\bar{V} = (\sqrt{4\pi k_B T/m})^3 / (\omega_x \omega_y \omega_z)$ is the mean volume of the atomic cloud, M is the mass of the Cr atoms, and $\beta_{dr} = \langle (\sigma_1 + 2\sigma_2) v_{rel} \rangle_{therm}$. Averaging over the interparticle velocities (v_{rel}), we consider that the atomic depolarization can occur via single or double spin-flips (σ_1 or σ_2). The measurement of $\beta_{dr} = 4 \pm 2 \times 10^{-13} \text{ cm}^3 \text{ s}^{-1}$ results in a good agreement with the theoretical predictions based on the first-order Born approximation for the dipole-dipole interaction ($\beta_{dr}[19 \mu\text{K}, 50 \text{ mG}] = 3.2 \times 10^{-13} \text{ cm}^3 \text{ s}^{-1}$; ref. 11).

Carrying out optical pumping following demagnetization is crucial for the preparation of the system before another cooling step using a smaller magnetic field to achieve a lower final temperature. This can be accomplished using σ^- polarized light on the $^7S_3 - ^7P_3$ optical dipole transition ($\lambda = 427$ nm). In this way, $m_j = -3$ is a dark state and its population is not affected by the pumping light. It is then possible to substitute several cooling steps by instead using a continuous ramp of the magnetic field while keeping the optical pumping beam (OPB) on during the whole sequence. It has been predicted theoretically that such a strategy should increase the cooling efficiency¹⁰.

To preserve the polarization of the OPB ($I_{\sigma^+}/I_{\sigma^-} \approx 1/1,000$), we must keep the external magnetic field aligned with respect to the OPB's propagation axis (y -axis). In fact, by minimizing the heating effect of the OPB on the atoms, we have been able to compensate residual magnetic fields B_x and B_z down to a few mG.

The continuous cooling sequence starts with 10^6 atoms at a temperature of 19 μ K and with $B_y = 250$ mG. The OPB is red-detuned by 40Γ ($\Gamma = 2\pi \times 5$ MHz) away from resonance and the total scattering rate is $\Gamma_{op} = 200$ photons per second. The best ramp of B_y , optimized experimentally to maximize the final phase-space density, results in a linear ramp down to 50 mG in 7 s. The temperature and atom number evolution can be seen in Fig. 3. The red circles allow for a comparison with the high magnetic field case. The final temperature is 11 μ K. The atom loss is not related to the cooling mechanisms, but is most probably due to the finite background gas pressure. The cooling is insensitive to the detuning of the OPB on both the red and the blue side of the resonance in the $2-40\Gamma$ interval. Lower temperatures have not been achieved by reducing B_y even further. In the next paragraph we discuss the possible limitations.

The atom light scattering is mainly coherent¹³ as long as we are using optical pumping that is widely detuned from resonance and the saturation parameter s is $\sim 10^{-5}$. Considering only the first-order process, the light re-emitted by the atoms is blue-shifted with respect to the pumping light by an amount $2\mu_B B$. Owing to the random direction of the emitted photon, every cooling

cycle causes an extra kick to the atoms with a total momentum $\hbar k$, where $k = 2\pi/\lambda$ is the light wavevector. However, simulations show that the ultimate temperature limit is slightly below the recoil temperature $T_{\text{rec}} = 1 \mu\text{K}$ (ref. 10). Reabsorption of the scattered photons could also be a serious limitation. The on-resonance light absorption cross-section $\sigma = 6\pi/k^2$ holds even if the fluorescence photon is far from resonance with the bare atom: in fact, the atoms are dressed by the optical pumping light and their fluorescence frequency matches the dressed states' energy difference¹⁴. Using the theoretical analysis presented in ref. 15, which is valid for $kr \geq 1$, where r is the interparticle separation, we can calculate the reabsorption probability. Note that the maximum density $n \sim 10^{13} \text{ atoms cm}^{-3}$ at the end of the cooling and the optical pumping wavevector k fulfil the $kr \geq 1$ condition. The reabsorption probability is

$$p \approx \frac{6\pi}{k^2} \frac{\Gamma_{\text{op}}}{\omega_{\text{D}}} \frac{1}{4\pi\langle r^2 \rangle} N.$$

The on-resonance cross-section is reduced by a factor $\Gamma_{\text{op}}/\omega_{\text{D}} \sim 10^{-4}$, where $\omega_{\text{D}} \sim 2 \times 10^5 \text{ s}^{-1}$ is the Doppler broadening at $10 \mu\text{K}$, $\langle r^2 \rangle$ is the mean square distance between two individual atoms in the trap ($\sim 3 \times 10^{-7} \text{ m}^2$) and $N \sim 10^6$ is the total number of trapped atoms. Consequently, for our experimental parameters the reabsorption probability is of the order of $p \sim 10^{-6}$. A theoretical analysis of the cooling including recoil energy, reabsorption, background gas and three-body collisions predicts a final temperature of $\sim 1 \mu\text{K}$ (ref. 10). We therefore conclude that a heating mechanism is currently limiting us, most probably coming from an imperfect control of the fields B_z and B_x . In fact, we observe a drift in the electrical currents that optimize such transversal fields. Several checks are necessary during a typical measurement day. This could be due to instability of our current generators or to random magnetization of our steel chamber during the switching of the magnetic trap that we use to prepare our atomic samples. External a.c. fields of the order of a few mG could also be a limiting factor.

The development of such a cooling technique helps us on our route towards the chromium Bose–Einstein condensate. Our measurements show that the efficiency of demagnetization cooling $\chi = -\ln(\rho_f/\rho_i)/\ln(N_f/N_i)$, which is associated with the gain in phase-space density ρ over the loss in atom number N , is larger than 11. So far, this is much better than the optimum value achieved (~ 4) using evaporative cooling. As a result of this, our starting conditions in the optical dipole trap are better, with nearly one order of magnitude higher phase-space density for the same atom number.

In the atom optics community, demagnetization cooling belongs to the family of laser cooling techniques in external fields^{16,17}. What is new is the mechanism that carries out the selection of higher-energy atoms. In our case, we make use of dipole–dipole inelastic collisions, whereas in other experiments this is carried out via optical Raman transitions^{18,19}. Such a technique, applied to Cs and carried out in a far-off-resonant lattice has led to a final phase-space density of $1/30$ (ref. 20). Higher values are prevented by inelastic hyperfine changing collisions occurring between two atoms at the same lattice site. Cr has no hyperfine structure and this will not be the limiting effect with regard to the challenge of achieving Bose–Einstein condensation via all-optical means using demagnetization cooling. As shown in ref. 21, a crucial requirement for the suppression of reabsorption will be to work in the *festina lente* regime, where reabsorption is prevented if the optical pumping rate Γ_{op} is smaller than the trapping frequency. Such a regime has been theoretically predicted to work if $kr \geq 1$ (ref. 15; at higher densities, radiative interatomic collisions start to play an important role²²). Considering our optical pumping light wavelength and the mass of Cr, we deduce that such a condition

is fulfilled for typical condensation temperatures below $3 \mu\text{K}$. An all-optical Bose–Einstein condensate with demagnetization cooling is then in principle possible with more accurate control of the external magnetic fields.

Demagnetization or general depolarization cooling is an important tool that can in principle be applied to all systems that exhibit the dipole–dipole interaction. However, it can only be useful when the inelastic collision rates are larger than the losses. Good candidates are rare-earth elements with large magnetic dipole moments (Dy, Ho, Eu, Tb, Er, Mo and so on)^{23,24} or molecules, either polar or non-polar but polarizable in the presence of an electric field²⁵. Although single-step depolarization has a cooling effect, to increase the phase-space density of the sample, an optical pumping transition is needed. Therefore, all atoms or molecules with an appropriate level structure can be used for this technique. Finally, note that as the dipole–dipole interaction is long range, in the partial wave decomposition of the cross-section, all the orders contribute, even in the limit of zero collision energy. Therefore, fermionic atoms and molecules can also demagnetize and thermalize via elastic dipole–dipole interaction.

Received 18 July 2006; accepted 2 October 2006; published 29 October 2006.

References

- Lounasmaa, O. V. *Experimental Principles and Methods Below 1 K* (Academic, New York, 1974).
- De Haas, W. J., Wiersma, E. C. & Kramers, H. A. Experiments on adiabatic cooling in paramagnetic salts in magnetic fields. *Physica* **1**, 1–13 (1934).
- Kurti, N., Robinson, F. N. H., Simon, F. & Spohr, D. A. Nuclear cooling. *Nature* **178**, 450–453 (1956).
- Oja, A. S. & Lounasmaa, O. V. Nuclear magnetic ordering in simple metals at positive and negative nanokelvin temperatures. *Rev. Mod. Phys.* **69**, 1–136 (1997).
- Touriniemi, J. T. & Knuutila, T. A. Nuclear cooling and spin properties of rhodium down to picokelvin temperatures. *Physica B* **280**, 474–478 (2000).
- Pecharsky, V. K. & Gschneidner, K. A. Giant magnetocaloric effect in Gd₅(Si₂Ge₂). *Phys. Rev. Lett.* **78**, 4494–4497 (1997).
- Morrish, A. H. *The Physical Principles of Magnetism* (Wiley, New York, 1983).
- Kastler, A. Quelques suggestions concernant la production optique et la détection optique d'une inégalité de population des niveaux de quantification spatiale des atomes. Application à l'expérience de Stern et Gerlach et à la résonance magnétique. *J. Phys. Radium* **11**, 255–265 (1950).
- Hänsch, T. W. & Schawlow, A. Cooling of gases by laser radiation. *Opt. Commun.* **13**, 68–69 (1975).
- Hensler, S., Greiner, A., Stuhler, J. & Pfau, T. Depolarisation cooling of an atomic cloud. *Europhys. Lett.* **71**, 918924 (2005).
- Hensler, S. et al. Dipolar relaxation in an ultra-cold gas of magnetically trapped chromium atoms. *Appl. Phys. B* **77**, 765–772 (2003).
- Griesmaier, A., Werner, J., Hensler, S., Stuhler, J. & Pfau, T. Bose–Einstein condensation of chromium. *Phys. Rev. Lett.* **94**, 160401 (2005).
- Cohen-Tannoudji, C., Dupont-Roc, J. & Grynberg, G. *Atom-Photon Interactions: Basic Processes and Applications* 382–383 (Wiley, New York, 1992).
- Olshani, M., Castin, Y. & Dalibard, J. in *Proc. 12th Int. Conf. Laser Spectroscopy* (eds Inguscio, M., Allegrini, M. & Sasso, A.) 7 (World Scientific, Singapore, 1996).
- Castin, Y. & Lewenstein, M. Reabsorption of light by trapped atoms. *Phys. Rev. Lett.* **80**, 5305–5308 (1998).
- Cirac, J. I. & Lewenstein, M. Cooling of atoms in external fields. *Phys. Rev. A* **52**, 4737–4740 (1995).
- Cirac, J. I., Lewenstein, M. & Zoller, P. Collective laser cooling of trapped atoms. *Europhys. Lett.* **35**, 647–651 (1996).
- Lee, H. J., Adams, C. S. & Chu, S. Raman cooling of atoms in an optical dipole trap. *Phys. Rev. Lett.* **76**, 2658–2661 (1996).
- Kerman, A. J., Vuletic, V., Chin, C. & Chu, S. Beyond optical molasses: 3D Raman sideband cooling of atomic cesium to high phase-space density. *Phys. Rev. Lett.* **84**, 439–442 (2000).
- Han, D. J. et al. 3D Raman sideband cooling of cesium atoms at high density. *Phys. Rev. Lett.* **85**, 724–727 (2000).
- Wolf, S., Oliver, S. J. & Weiss, D. S. Suppression of recoil heating by an optical lattice. *Phys. Rev. Lett.* **85**, 4249–4252 (2000).
- Hijmans, T. W. & Burin, A. L. Influence of radiative interatomic collisions on dark-state cooling. *Phys. Rev. A* **54**, 4332–4338 (1996).
- Hancox, C. I., Doret, S. C., Hummon, M. T., Luo, L. & Doyle, J. M. Magnetic trapping of rare-earth atoms at millikelvin temperatures. *Nature* **431**, 281–284 (2004).
- McClelland, J. J. & Hanssen, J. L. Laser cooling without repumping: A magneto-optical trap for erbium atoms. *Phys. Rev. Lett.* **96**, 143005 (2006).
- Friedrich, B. & Herschbach, D. Statistical mechanics of pendular molecules. *Int. Rev. Phys. Chem.* **15**, 325–344 (1996).

Acknowledgements

We thank our atom optics group for encouragement and practical help. We thank G. J. Birnir for careful reading of the manuscript. This work was supported by the German Science Foundation (DFG) (SPP1116 and SFB/TR 21).

Correspondence and requests for materials should be addressed to M.F. or T.P.

Author contributions

M.F., T.K. and S.G. carried out the experimental work and data analysis, A.G. carried out experimental work and S.H., J.S. and T.P. were responsible for project planning.

Competing financial interests

The authors declare that they have no competing financial interests.

Reprints and permission information is available online at <http://npg.nature.com/reprintsandpermissions/>